**acta physica slovaca vol. 56 No. 4, 511 – 520** **August 2006**

# MELTING OF $Au_N$ ($N = 12, 13, 14$) MICROCLUSTERS

**H. Arslan**[1], **M.H.Guven**[2]
*Zonguldak Karaelmas University, Department of Physics, 67100 Zonguldak, Turkey*

Received 23 May 2005, in final form 5 December 2005, accepted 26 January 2006

The melting properties of $Au_N$ ($N = 12, 13, 14$) clusters have been investigated by constant energy Molecular Dynamics and Monte Carlo simulations on the basis of Sutton Chen potential. The minimum energy geometries of $Au_{12}$ and $Au_{14}$ are interesting because they are not ico-based in contrast to the other metal clusters with the same size. The melting temperatures of the clusters are reported and compared with the values given in the literature. Considerable reduction in the melting temperatures of the clusters has been found. The premelting stage of $Au_{14}$ is observed.

PACS: 36.40.Ei, 36.40.Qv

## 1 Introduction

The investigation of small atomic and molecular clusters is an active area of current research, both theoretically [1–8] and experimentally [9–14]. The physical and chemical properties of these clusters are found to be different from the bulk. Their structures, electronic, magnetic and chemical properties are different from those of bulk and depend on size non-monotonically [11,15,16]. The most fundamental property of a cluster is its unique minimum energy geometry. To achieve a deeper understanding of the physical mechanism responsible for the structural, dynamical and thermodynamics of clusters, some authors [17–19] have investigated the influence of the nature of the inter atomic interactions on the behaviours of the clusters. One major motivation for the study of clusters is the insight that can be provided for understanding the transition from finite to bulk behaviour. The melting transition in the clusters has also different from the bulk and subject of intense research activity [5, 8]. Due to the fact that in small particles most of the atoms are located on the surface, the clusters have lower melting temperatures and the phase transition is spread over a finite temperature range [11, 12].

Theoretical modelling is important to interpret the experimental data for understanding the properties and mechanisms of the cluster dynamics. Performing ab initio calculations for transition metal clusters, even for their structure determination, is limited to structures of high symmetry [20–22]. Instead, model potentials are used in molecular dynamics (MD) and Monte Carlo (MC) simulations for mimicking the inter atomic interactions. Delocalisation of electrons in the

[1]E-mail address: arslan@karaelmas.edu.tr
[2]E-mail address: haluk_guven@yahoo.com

metals leads to an important role of the many body effects. Therefore modelling of these effects is a challenging task.

Some groups have studied the 13-particle clusters, which have the extremely stable ground state icosahedral structure and thus offer a particular clear case for the study of the rigid to nonrigid transition. Lee and co-workers [7] presented an atom-resolved analysis of surface melting in $Ni_N$ ($N$=12–14)clusters modelled by tight binding method by using the standard Monte Carlo simulation technique. Sebetci and co-workers [6] presented an atom-resolved analysis of temperature-depended behaviours of $Pt_N$ ($N$=12–14) clusters modelled by the Voter-Chen version of the Embedded Atom Model potential by employing in the Molecular Dynamics (MD) simulations. In this study, we present the results of both molecular dynamics and Monte Carlo study of the melting of $Au_N$ ($N$=12–14) clusters modelled by the Sutton-Chen potential and the results are compared with the predictions obtained from the Gupta potentials and Sutton-Chen potentials. The potential and the computational details are presented in Section 2. The results and their discussions are given in Section 3. We summarised our results in Section 4.

## 2 Potential and Methodology

The Sutton-Chen potential has the form [23]

$$E = \varepsilon \left[ \frac{1}{2} \sum_i \sum_{j \neq i} V(r_{ij}) - c \sum_i \sqrt{\rho_i} \right], \tag{1}$$

where

$$V(r_{ij}) = \left( \frac{a}{r_{ij}} \right)^n, \qquad \rho_i = \sum_{j \neq i} \left( \frac{a}{r_{ij}} \right)^m. \tag{2}$$

Here $r_{ij}$ is the separation between atoms $i$ and $j$, $c$ is a positive dimensionless parameter, $\varepsilon$ is a parameter with dimensions of energy, $a$ is a parameter with the dimensions of length, $m$ and $n$ are positive integers. We use the same parameters given by Sutton and Chen [23] for Au and $n = 10$, $m = 8$, $c = 34.408$,$\varepsilon = 1.2793 \times 10^{-2}$ eV and, $a = 4.08$ Å. This potential has been shown to reproduce bulk and surface properties quite accurately as reported in references [24–26] and references therein.

The structural properties of $Au_N$ (N containing up to 80 atoms) clusters that are modeled by the Sutton-Chen potential, have been investigated using a MC minimisation approach and the global minima are reported [26]. The coordinates of the minima are available in downloadable form from the Cambridge Cluster Database [27].

The isomer distribution of $Au_N$ ($N$=12,13,14) clusters are studied by eigenvector-following technique [28, 29]. To obtain all the isomers of clusters, $5 \times 10^3$ distinct random configurations for each cluster size were prepared. Then these sets of random configurations were optimized by eigenvector-following technique. This procedure is repeated for the new sets of distinct random configurations and it is stopped when the total number of isomers of each cluster remains constant. It is observed that $3 \times 10^4$ random configurations for $Au_{12}$, $6 \times 10^4$ random configurations for $Au_{13}$ and $8 \times 10^4$ random configurations for $Au_{14}$ are seen enough to determine the

Tab. 1. The binding energy (BE) (eV/Atom) and point groups (PG) of global minimum and first five isomers of $Au_N$ (N=12,13,14) clusters.

| | $Au_{12}$ | | $Au_{13}$ | | $Au_{14}$ | |
|---|---|---|---|---|---|---|
| | BE [eV/Atom] | PG | BE [eV/Atom] | PG | BE [eV/Atom] | PG |
| Global Minimum | $-3.2045$ | $C_2$ | $-3.2281$ | $I_h$ | $-3.2433$ | $C_{6v}$ |
| Isomer1 | $-3.2039$ | $D_{2d}$ | $-3.2195$ | $C_s$ | $-3.2380$ | $C_2$ |
| Isomer2 | $-3.2031$ | $D_{3h}$ | $-3.2177$ | $C_{3v}$ | $-3.2378$ | $C_s$ |
| Isomer3 | $-3.2016$ | $C_s$ | $-3.2171$ | $C_2$ | $-3.2372$ | $C_s$ |
| Isomer4 | $-3.2006$ | $C_1$ | $-3.2170$ | $C_s$ | $-3.2358$ | $C_s$ |
| Isomer5 | $-3.1996$ | $C_1$ | $-3.2163$ | $C_{2v}$ | $-3.2357$ | $C_s$ |

all isomers of those clusters as far as the eigenvector-following techniques is concerned. During the optimization process, binding energy and point groups of clusters are obtained and global minimum and first five isomers of clusters are listed in Table 1.

To investigate the melting properties of $Au_N$ ($N$=12,13,14) clusters, the Hamiltonian equations of motions are solved by the Sutton - Chen potential for all the atoms in a cluster on a grid of total energies using Hamming's modified fourth order predictor corrector propagator with a step size of $0.5 \times 10^{-15}$ s. The clusters are prepared with zero initial total linear and angular momenta. Then, the clusters are gradually heated. Trajectories of length of $5 \times 10^5$ steps are generated on a grid of total energies large enough to observe the solid liquid transition in the cluster. The total energy in the individual runs is conserved within $0.001\%$. To analyse the cluster melting in MD simulations, the relative root mean square (RMS) bond length fluctuation and diffusion coefficients as a function of temperature are calculated.

Thermodynamic properties of the $Au_N$ ($N$=12,13,14) clusters are calculated with Monte Carlo methods using the parallel tempering technique [30,31,32]. In the parallel tempering scheme a number of simulation boxes are run simultaneously, each one at a different total energy for the microcanonical case. Parallel tempering Monte Carlo is specially designed to overcome ergodicity breaking problems that occur when two or more local minima are separated by high potential barriers. Using the parallel tempering method, we have run for a set of 30 total energies ranging from $-38.3514$ eV to $-35.3528$ eV for $Au_{12}$, $-41.7439$ eV to $-37.6209$ eV for $Au_{13}$ and $-45.2524$ eV to $-40.7545$ eV for $Au_{14}$. The simulations are begun with randomly initialized configurations and $10^6$ Metropolis Monte Carlo points (no exchanges) followed by $5 \times 10^6$ parallel tempering Monte Carlo points.

## 3 Results and Discussion

The structures of $Au_N$ ($N$=12,13,14) clusters are reported in the literature by Jellinek and Wales groups using the Gupta potential and Sutton-Chen potential respectively [33–36]. Both groups agree that the global minimum of $Au_{13}$ is a complete icosahedrons and the most stable structures of $Au_{12}$ and $Au_{14}$ are not ico-based [33]. In contrast, the most stable structures of small nickel and palladium clusters, including $Ni_{12}$, $Ni_{14}$, $Pd_{12}$, and $Pd_{14}$ are ico-based.

As a result of the isomer distribution calculations, we have obtained $407$ isomers for $Au_{12}$, $1347$ isomers for $Au_{13}$ and $3724$ isomers for $Au_{14}$. When we consider the energy spectrum

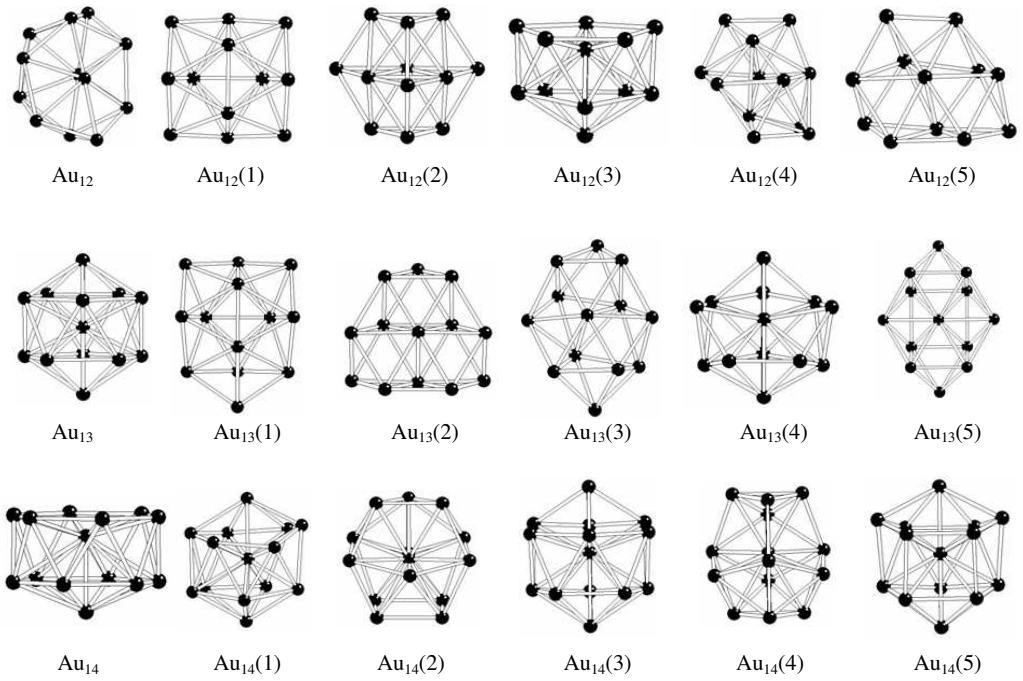


Fig. 1. The global minimum and first five isomer geometries of the $Au_N$ ($N$=12,13,14) clusters

of the $Au_N$ ($N$=12,13,14) clusters, the energy gap between the global minimum and the next higher energy isomers are very small. It is found that, the energy difference between the global minimum and the first isomer is $0.00066$ eV/Atom for $Au_{12}$, $0.00860$ eV/Atom for $Au_{13}$ and $0.00534$ eV/Atom for $Au_{14}$ as presented in Table 1. On the other hand, the energy spectrum widths, ESW, (the energy difference between the lowest and the highest energy isomers) are in the order of $Au_{14} > Au_{13} > Au_{12}$. The global minimum and first five isomer geometries of the clusters are presented in Fig. 1.

In order to investigate the melting dynamics of the $Au_N$ (N=12,13,14) clusters, the root mean square (RMS) bond length fluctuations for three clusters are displayed in Fig. 2. The $\delta$ graph is the most important graph to observe the melting-like transition of the clusters. As it is seen from the Fig. 2, the relative root mean square deviation of nearest neighbour distances is less than $0.1$ for solid regions and well above $0.1$ for liquid regions. The $\delta$ graph of $Au_{14}$ cluster shows characteristic shape of premelting. The jump of the $\delta$ values of $Au_{14}$ in a very narrow temperature range is due to the high mobility of the surface atoms. However, the core melts at higher temperatures. The $Au_{13}$ cluster, which has a stable icosahedral structure, melts as a whole in a finite range of temperature. The change in $\delta$ curve of $Au_{12}$ is not as abrupt as in the cases the other clusters; we think that this is due to its glassy structure.

To corroborate the melting type nature of the transition, the diffusion coefficients are displayed as a function of temperatures respectively for three clusters in Fig. 3. The diffusion coef-

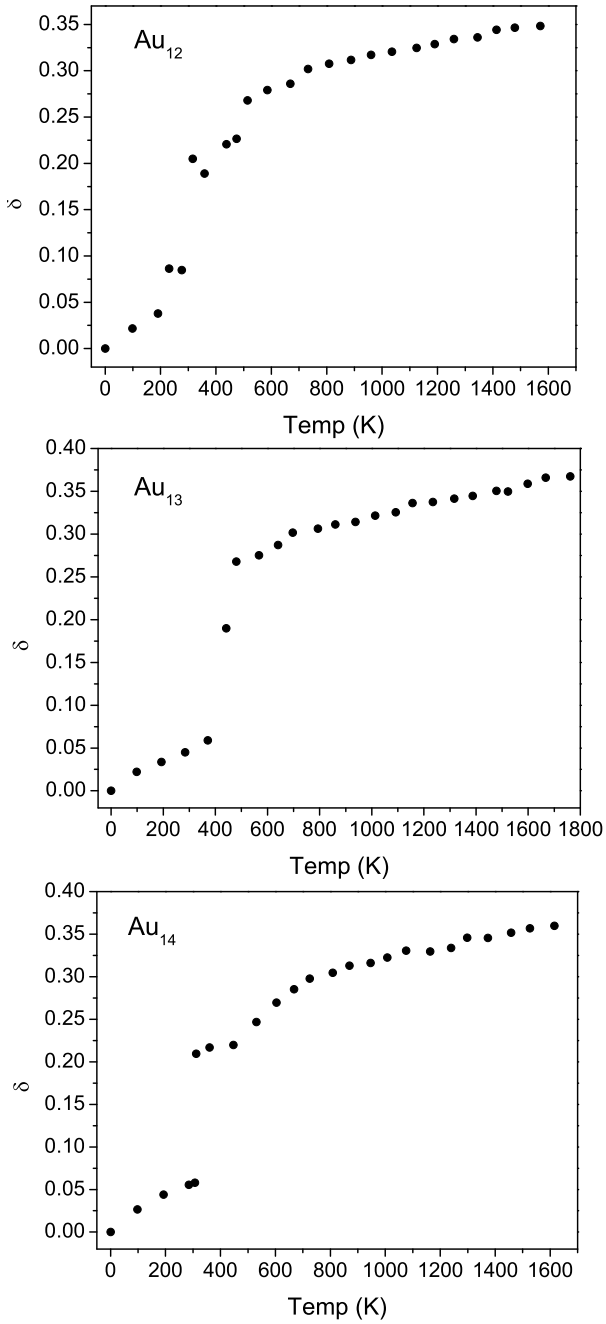


Fig. 2. Root-mean-square bond length fluctuations of $Au_N$ ($N$=12,13,14) clusters as a function of temperature.

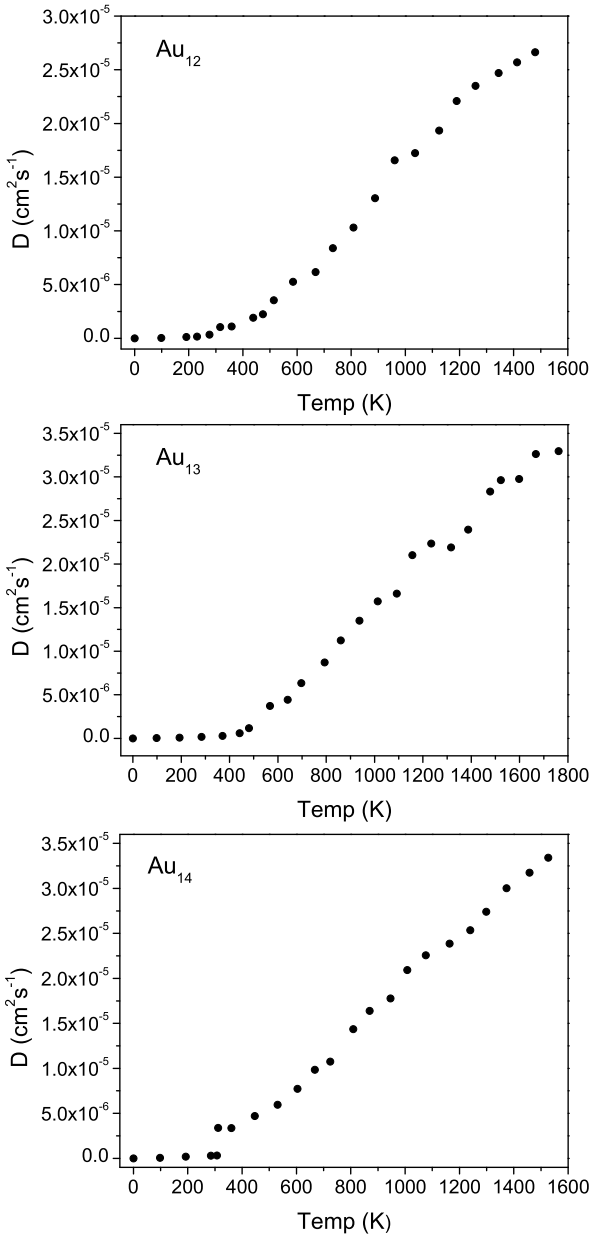


Fig. 3. Diffusion coefficient of $Au_N$ ($N$=12,13,14) clusters as a function of temperature.

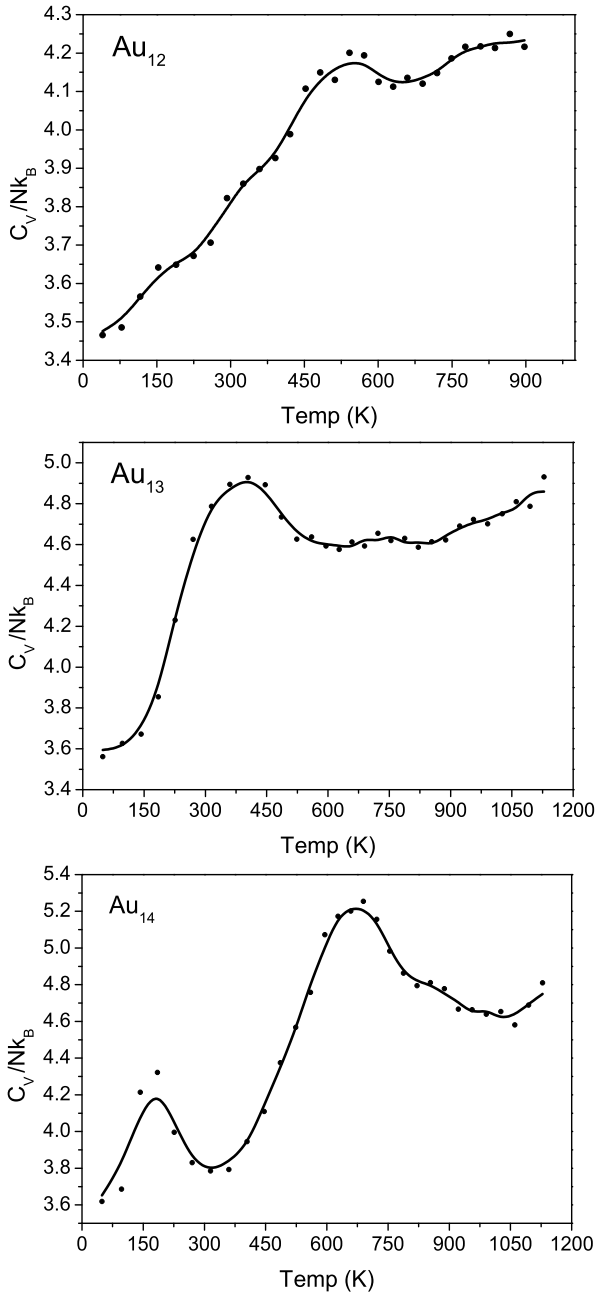


Fig. 4. Heat capacity ($C_v$) curves of $Au_N$ ($N$=12,13,14) clusters. $N$ is the number of atoms and $k_B$ is the Boltzmann constant.

ficients for $Au_N$ ($N$=12,13,14) clusters remain nearly zero at the beginning that corresponding to rigid like structures. After a certain temperatures, the diffusional motion only begins to develop. In the case of $Au_{14}$ cluster, there is a jump in diffusion coefficient at temperatures about $300$ K that corresponds to premelting temperatures. When the diffusional motion begins to develop, the variation of diffusion coefficient as a function of temperatures is almost linear as seen in Fig. 3. It is concluded that the increase in diffusion coefficients for $Au_N$ ($N$=12,13,14) clusters is an indicator of the phase transitions.

We have presented the heat capacity ($C_v$ curves of $Au_N$ ($N$=12,13,14) clusters in Fig. 4. The slope of the curve $Au_{12}$ cluster begins to increase near $0$ K and it increases continuously up to $550$ K, which correspond to the fully liquid phase of the cluster and do not coincide with the temperature at which the RMS bond length fluctuation increase rapidly. For $Au_{13}$ cluster, the phase changes start at about $200$ K and the cluster is in the fully liquid phase about $400$ K, where the increase in the slope of the heat capacity curve vanishes. This temperature is very close to the temperature of RMS bond length fluctuation increase rapidly. On the other hand, the melting behaviour of the $Au_{14}$ cluster is different from the previous two clusters $Au_{12}$ and $Au_{13}$. Heat capacity curve of $Au_{14}$ cluster shows two stage melting behaviour as seen in RMS bond length fluctuation curve. For $Au_{14}$ cluster, the peak at low temperature is due to the premelting, and the peak at higher temperature is due to the overall melting. For $Ni_{12}$ and $Ni_{14}$ clusters, Lee and co-workers also obtained premelting stage for RMS bond length fluctuation calculations, but they did not get the premelting stage for those clusters using the standard Metropolis Monte Carlo simulations [7]. Sebetci and co-workers have obtained premelting stage for $Pt_{14}$ for both RMS bond length fluctuation and standard Metropolis Monte Carlo simulations [6]. Gallego and co-workers reported the melting temperatures of $Au_{13}$, as $413$ K by using Tight Binding Model 1 (Gupta potential) and as $247$ K using Embedded Atom Model 1 [18]. Jellinek and co-workers, using the Gupta potential with different parameterisation, found the melting temperatures of $Au_{12}$, $Au_{13}$, and $Au_{14}$ as $460$ K, $680$ K and $440$ K respectively [34, 35]. Then these values are corrected in reference (31) of reference [33] that given values should be divided by 2. In this study, the melting temperature of $Au_{13}$ is higher the melting temperatures of $Au_{12}$ and $Au_{14}$ (as we consider the premelting). This is also an indication of the stable structure of the $Au_{13}$ compared to the other clusters. Our MD and PTMC simulations prove that the melting temperatures of the clusters are reduced considerably compared to the bulk melting temperatures of gold, which is $1338$ K. The reduction is approximately about $30\%$. The melting temperatures ($T_m$) of clusters are determined from RMS bond length fluctuation curve (according to Lindemann criterion, i.e.$\delta \approx 0.18$) and heat capacity curve, as presented in Table 2.

Tab. 2. Melting (premelting) temperatures ($T_m$) of $Au_N$ (N=12,13,14) clusters.

| Cluster | $T_m$(K) (MD) | $T_m$(K) (MC) |
|---|---|---|
| $Au_{12}$ | 320 | 540 |
| $Au_{13}$ | 445 | 400 |
| $Au_{14}$ | 295 (premelting)<br>680 (overall melting) | 180 (premelting)<br>695 (overall melting) |

The difference between the calculated melting temperatures in this study and those of given in literature is due to the model potential function used in the calculations. Even the same potential functions with different parameterizations gives different results [18, 34, 35]. According to experimental results the model potentials could be re parameterized. Therefore, to mimic the inter atomic interactions more realistic, cluster experimental data is required.

## 4 Conclusion

The melting dynamics of small gold clusters were investigated with both classical molecular dynamics and Monte Carlo simulations. For this reason, morphologically interesting three clusters $Au_{12}$, $Au_{13}$ and $Au_{14}$ have been investigated by employing Sutton-Chen potential which is based on the tight binding model and have been applied to metallic clusters successfully. The minimum energy geometry of $Au_{13}$ is an icosahedron but $Au_{12}$ and $Au_{14}$ are not ico-based, i.e., the gold clusters favours glass-like structures. Gold clusters modelled with Sutton-Chen potential which has attractive part and effective in short ranges. Therefore, they have very many isomers with extremely small energy differences. Isomers energy spectrum widths are calculated and we conclude that as the number of the stable isomers increases the energy spectrum widths also increases and the order of widths are $Au_{14} > Au_{13} > Au_{12}$.

During the melting process, $Au_{12}$ undergoes isomerisation at very low temperatures due to its glassy structure. If we compare the Lindemann curve and heat capacity curve of $Au_N$ (N=12,13,14) clusters, it is obvious that both curve of $Au_{12}$ cluster show similar behaviour and these curves grow up gradually in wide range of temperature. In the case of $Au_{13}$, there is a sudden increase in Lindemann and heat capacity curves. It is also found that the energy difference between the global minimum and the next higher isomer is largest in $Au_{13}$ cluster compared to other clusters. In this sense it is concluded that $Au_{13}$ cluster is more stable than $Au_{12}$ and $Au_{14}$. In the case of $Au_{14}$, the premelting stage is observed for both molecular dynamics and parallel tempering Monte Carlo calculations. The reductions in melting temperatures of clusters compared to the bulk melting temperatures are about $30\%$.

### References


[1] J. Jellinek: *Theory of Atoms and Molecular Clusters*. Ed. J. Jellinek, Springer, Berlin 1999

[2] H. Haberland:*Clusters of Atoms and Molecules I: Theory, Experiment and Clusters of Atoms.* Springer Verlag: New York 1995

[3] M.H. Guven, M. Eryurek: *Phys. Stat. Sol. (b)* **213** (1999) 283

[4] N.T. Wilson, R.L. Johnston: *Eur. Phys. J. D* **12** (2000) 161

[5] M. Karabacak, S. Ozcelik, Z.B. Guvenc: *Acta Phys. Slov.* **54** (2004) 233

[6] A. Sebetci, Z.B. Guvenc: *Modelling Simul. Mater. Sci. Eng.* **12** (2004) 1131

[7] Y.J. Lee, J.Y. Maeng, E.K. Lee, B. Kim, S. Kim, K-K. Han: *J. Comp. Chem* **21** (2000) 380

[8] H. Arslan, M.H. Guven: *New J. Phys.* **7** (2005) 60

[9] E.K. Parks, K.P. Kerns, S.J. Riley: *Chem. Phys.* **262** (2000) 151

[10] C.L. Cleveland, U. Landman, J.G. Schaaff, M.N. Shafigullin, P.W. Stephens, R.L. Whetten: *Phys. Rev. Lett.* **79** (1997) 1873

[11] M. Schmidt, R. Kusche, B.v Issendorf, H. Haberland: *Nature (London)* **393** (1998) 238

[12] M. Schmidt, R. Kusche, W. Kronmller, B.v Issendorf, H. Haberland: *Phys. Rev. Lett.* **79** (1997) 99

[13] M.Y. Efremov, F. Schiettekatte, M. Zhang, E.A. Olson, A.T. Kwan, R.S. Berry, L.H. Allen: *Phys. Rev. Lett.* **85** (2000) 3560

[14] M. Schmidt, J. Donger, Th. Hippler, H. Haberland: *Phys. Rev. Lett* **90** (1998) 103401

[15] T.L. Beck, J. Jellinek, R.S. Bery: *J. Chem. Phys.* **87** (1987) 545

[16] F. Calvo, F. Spiegelman: *J. Chem. Phys.* **112** (2000) 2888

[17] A. Cheng, M.L. Klein, C. Caccamo: *Phys. Rev. Lett.* **71** (1993) 1200

[18] C. Rey, L.J. Gallego, J. Garcia-Rodeja: *Phys. Rev. B* **48** (1993) 8253

[19] C. Rey, J. Garcia-Rodeja, L.J. Gallego: *Phys. Rev. E* **57** (1998) 4420

[20] B.V. Reddy, S.K. Nayak, S.N. Khanna, B.K Rao, P. Jena: *J. Phys. Chem. A* **102** (1998) 1748

[21] O.D. Hberlen, S.C. Chung, M. Stener, N. Rsch: *J.Chem.Phys.* **106** (1997) 5189

[22] J. Wang, G. Wang, J. Zhao: *Phys. Rev. B* **66** (2002) 035418

[23] A.P. Sutton, J. Chen: *Philos. Mag. Lett.* **61** (1990) 139

[24] S.H.Nayak, S.N. Khanna, B.K. Rao, P. Jena: *J. Phys.: Cond. Mat.* **10** (1998) 10853

[25] B.D. Todd, R.M. Lynden-Bell: *Surf. Sci.* **281** (1993) 191

[26] J.P.K. Doye, D.J. Wales: *New J. Chem.* **773** (1998)

[27] D.J. Wales, J.P.K. Doye, A. Dullweber, F.Y. Naumkin: *The Cambridge Cluster Database (1998), URL: http://brian.ch.cam.ac.uk/CCD.html*

[28] C.J. Cerjan, W.H. Miller: *J. Chem. Phys.* **75** (1981) 2800

[29] J.P.K. Doye, D.J. Wales: *Z. Phys. D* **40** (1997) 194

[30] J.P. Neirotti, F. Calvo, D.L. Freeman, J.D. Doll: *J. Chem. Phys.* **112** (2000) 10340

[31] F. Calvo, J.P. Neirotti, D.L. Freeman, J.D. Doll: *J. Chem. Phys.* **112** (2000) 10350

[32] M.A. Carignano: *Phys. Lett.* **361** (2002) 291

[33] J. Jellinek: *Metal - Ligand Interactions*: , **e** (d) . N. Russo ,D.R. Salahub;Kluwer Academic Publishers, The Nederlands 1996

[34] I.L. Garzon, J. Jellinek: *Z. Phys. D* **20** (1991) 235

[35] I.L. Garzon, J. Jellinek: *Z. Phys. D* **26** (1993) 316

[36] J. Uppenbrink, D.J. Wales: *J. Chem. Phys.* **98** (1993) 5720